nature genetics

Mutations in the gene encoding GlyT2 (*SLC6A5*) define a presynaptic component of human startle disease

Mark I Rees[1,3,14], Kirsten Harvey[2,14], Brian R Pearce[2], Seo-Kyung Chung[1,3], Ian C Duguid[4], Philip Thomas[4], Sarah Beatty[3], Gail E Graham[5], Linlea Armstrong[6], Rita Shiang[7], Kim J Abbott[8], Sameer M Zuberi[9], John B P Stephenson[9], Michael J Owen[10], Marina A J Tijssen[11], Arn M J M van den Maagdenberg[12], Trevor G Smart[4], Stéphane Supplisson[13] & Robert J Harvey[2]

Hyperekplexia is a human neurological disorder characterized by an excessive startle response and is typically caused by missense and nonsense mutations in the gene encoding the inhibitory glycine receptor (GlyR) α1 subunit (*GLRA1*)[1–3]. Genetic heterogeneity has been confirmed in rare sporadic cases, with mutations affecting other postsynaptic glycinergic proteins including the GlyR β subunit (*GLRB*)[4], gephyrin (*GPHN*)[5] and RhoGEF collybistin (*ARHGEF9*)[6]. However, many individuals diagnosed with sporadic hyperekplexia do not carry mutations in these genes[2–7]. Here we show that missense, nonsense and frameshift mutations in *SLC6A5* (ref. 8), encoding the presynaptic glycine transporter 2 (GlyT2), also cause hyperekplexia. Individuals with mutations in *SLC6A5* present with hypertonia, an exaggerated startle response to tactile or acoustic stimuli, and life-threatening neonatal apnea episodes. *SLC6A5* mutations result in defective subcellular GlyT2 localization, decreased glycine uptake or both, with selected mutations affecting predicted glycine and Na^+ binding sites.

Glycine transporters (GlyTs) are members of the Na^+/Cl^--dependent neurotransmitter transporter superfamily[9,10], integral membrane proteins that use electrochemical gradients to control the concentration of neurotransmitters at central synapses. This superfamily also includes transporters for GABA, biogenic amines (norepinephrine, dopamine, serotonin and proline), betaine, taurine and creatine. GlyTs have dual functions at both inhibitory and excitatory synapses, resulting from the differential localization of two distinct transporters[9,10], GlyT1 and GlyT2. GlyT1 is predominantly expressed in glial cells[9,10] and shows a stoichiometry of 2 Na^+/1 Cl^-/1 glycine and bidirectional glycine transport[11]. These properties are appropriate for the control of extracellular glycine concentrations in the submicromolar range for modulation of *N*-methyl-D-aspartate receptors[12] and also for lowering extracellular glycine levels at inhibitory glycinergic synapses[13,14]. By contrast, GlyT2 is found in glycinergic axons, shows a stoichiometry of 3 Na^+/1 Cl^-/1 glycine and does not show reverse uptake[11], reflecting an essential role for GlyT2 in maintaining a high presynaptic pool of neurotransmitter at glycinergic synapses[15]. Na^+/Cl^--dependent transporters are known targets for therapeutic drugs (for example, anticonvulsants[16] and selective serotonin reuptake inhibitors[17]) and for drugs of abuse (for example, cocaine and amphetamine). For this reason, genetic variation in human transporter genes has been studied in a variety of disorders including Parkinson disease[18], depression[18], orthostatic intolerance[19] and epilepsy[20]. Although mutations in the human creatine transporter gene (*SLC6A8*) on chromosome Xq28 are associated with mental retardation[21,22], no genetic defects in classical Na^+/Cl^--dependent neurotransmitter transporters (GABA, serotonin and glycine) have been directly related to human disorders. Nevertheless, we considered that neurological disorders with a postsynaptic genetic component might also have a corresponding undiscovered presynaptic defect. For example, hereditary hyperekplexia (OMIM 149400) is a rare but potentially lethal condition, typically caused by mutations in the gene encoding the glycine receptor (GlyR) α1 subunit (*GLRA1*)[1–3]. Despite isolated hyperekplexia cases with mutations affecting the GlyR β subunit (*GLRB*)[4] and the clustering proteins gephyrin (*GPHN*)[5] and collybistin (*ARHGEF9*)[6], for many individuals with sporadic hyperekplexia no causative mutation has been

[1]School of Medicine, University of Wales Swansea, Singleton Park, West Glamorgan SA2 8PP, UK. [2]Department of Pharmacology, The School of Pharmacy, 29–39 Brunswick Square, London WC1N 1AX, UK. [3]Department of Molecular Medicine, Faculty of Medical and Health Sciences, University of Auckland, Private bag 92019, Auckland, New Zealand. [4]Department of Pharmacology, University College London, Gower Street, London WC1E 6BT, UK. [5]Department of Genetics, Children's Hospital of Eastern Ontario, 401 Smyth Road, Ontario K1H 8L1, Canada. [6]Department of Medical Genetics, Children's and Women's Health Centre of British Columbia, 4500 Oak Street, Vancouver, British Columbia V6H 3N1, Canada. [7]Department of Human Genetics, Virginia Commonwealth University Medical Center, P.O. Box 980033, Richmond, Virginia 23298-0033, USA. [8]Women's and Children's Hospital, 72 King William Road, Adelaide, South Australia, Australia. [9]Fraser of Allander Neurosciences Unit, Royal Hospital for Sick Children, Glasgow, G3 8SJ, UK. [10]Psychological Medicine, University of Wales College of Medicine, Cardiff CF14 4XN, UK. [11]Department of Neurology, Academic Medical Centre, University of Amsterdam, PO BOX 22660, 1100 DD Amsterdam, The Netherlands. [12]Department of Neurology and Department of Human Genetics, Leiden University Medical Centre, PO Box 9600, 2300 RC Leiden, The Netherlands. [13]Laboratoire de Neurobiologie, CNRS UMR8544, Ecole Normale Supérieure, 46 Rue d'Ulm, 75005 Paris, France. [14]These authors contributed equally to this work. Correspondence should be addressed to R.J.H. (robert.harvey@pharmacy.ac.uk) or M.I.R. (m.i.rees@swansea.ac.uk).

Received 13 December 2005; accepted 5 May 2006; published online 4 June 2006; doi:10.1038/ng1814

Table 1 Mutations in *SLC6A5* in individuals with hyperekplexia

Individual	Global origin	Parental origin	Sequence change	Exon	Amino acid alteration	Subcellular location	Glycine transport	Mechanism
1	Canada	Paternal	C1131A	7	Y377X	Cytoplasmic	Abolished	In-frame stop codon, protein truncation
		Maternal	G1294T + Ins[T]1295	8	V432F+fs97	Cytoplasmic	Abolished	Missense plus frameshift, protein truncation
2	USA	Unknown	A1472G	9	Y491C	Cell surface	Abolished	Missense, functionally inert
			C1888T	13	Q630X	Cytoplasmic	Abolished	In-frame stop codon, protein truncation
3	Australia	Unknown	delC{319–324}	2	P108L+fs25	Cytoplasmic	Abolished	Missense plus frameshift, protein truncation
			T1444C	9	W482R	Cell surface	Abolished	Missense, glycine-binding site (W482R)
4	Netherlands	Paternal	C916G	5	L306V	Cell surface	Abolished in	Missense, sodium-binding site (N509S),
		Maternal	A1526G	10	N509S	Cell surface	L306V+N509S	compound recessive
5	Netherlands	Paternal	C1274T	8	T425M	Cell surface	Abolished	Missense, functionally inert
		Maternal	C1274T	8	T425M			
6	UK	Maternal	T1530G	10	S510R	Cytoplasmic	Abolished	Missense mutation, S510R forms large intracellular aggregates, dominant-negative

identified[2–7]. Because knockout mice for the presynaptic Na^+/Cl^--dependent transporter GlyT2 have been reported[15] to show a phenotype similar to hyperekplexia, as part of a continuing screening program we assessed whether defects in *SLC6A5*, encoding human GlyT2, could cause this disorder.

We scanned all 16 coding exons of *SLC6A5* (11p15.1) by denaturing high-performance liquid chromatography (dHPLC) (for primers see **Supplementary Table 1** online) in an international cohort of 83 individuals with sporadic or familial hyperekplexia[2–7] devoid of mutations in *GLRA1*, *GLRB*, *GPHN* and *ARHGEF9* (**Supplementary Table 2** online). Direct sequencing of aberrant dHPLC profiles revealed a mosaic of missense and nonsense mutations in *SLC6A5* (**Table 1**, **Fig. 1** and **Supplementary Fig. 1** online) and further regions of common SNPs (**Supplementary Table 3** online). All mutations in **Table 1** were absent from 400 unrelated, normal control chromosomes. In most cases (five of six), *SLC6A5* mutations were inherited as compound heterozygotes or as homozygotes, indicating that *SLC6A5* is predominantly associated with recessive hyperekplexia (**Table 1** and **Fig. 1**). A nonsense mutation (resulting in the alteration Y377X) plus a mixed missense and frameshift mutation (resulting in the alteration V432F+fs97) were present in individual 1, who is severely affected and with compound inheritance of null alleles. In the mother, the V432F+fs97-causing mutation segregated with a partial form of hyperekplexia, associated with nocturnal myoclonus and a nervous

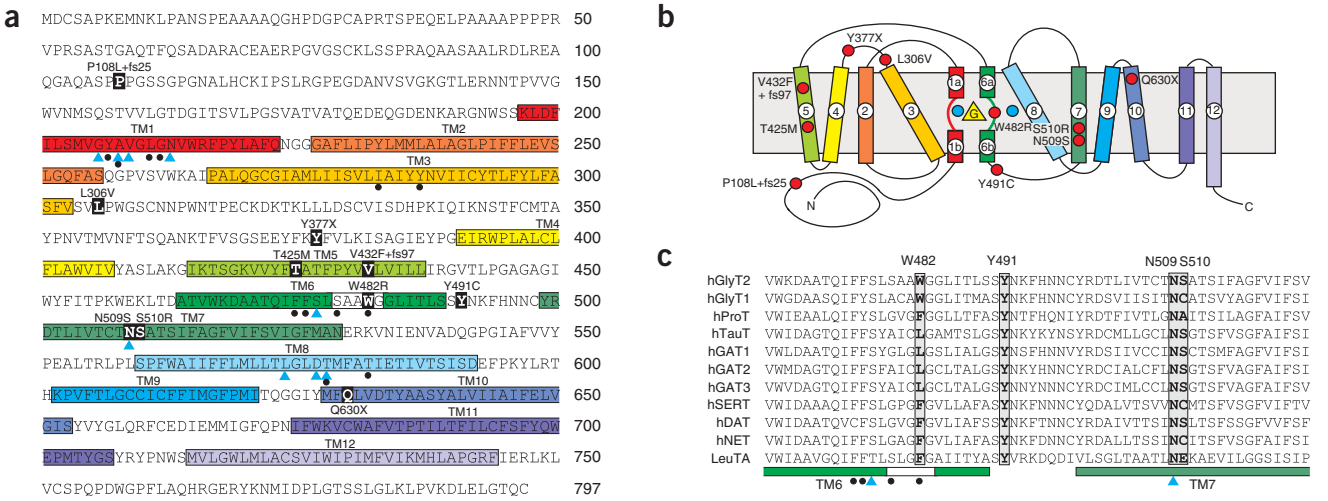

Figure 1 Amino acid sequence of human GlyT2 indicating alterations identified in hyperekplexia. (**a**) Amino acid sequence of human GlyT2 indicating the revised positions of putative transmembrane (TM) domains (colored boxes). Blue triangles show residues in hGlyT2 that are likely to coordinate Na^+ ions based on sequence alignments with the bacterial leucine transporter LeuT (ref. 24). This involves residues in TM1 (Gly206, Ala208, Val209, Asn213), TM6 (Ser477), TM7 (Asn509) and TM8 (Lys574, Asp577, Thr578). However, it is noteworthy that GlyT2 binds three Na^+ ions, whereas LeuT binds two, suggesting that other residues involved in Na^+ coordination remain to be identified. Filled black circles indicate residues predicted to be involved in glycine binding, including residues in TM1 (Tyr207, Ala208, Lys211, Gly212), TM3 (Ile283, Tyr287), TM6 (Phe475, Phe476, Ser479, Trp482) and TM8 (Thr578, Thr582). (**b**) Schematic diagram showing the suggested topology of GlyT2 and relative positions of GlyT2 alterations (red circles), adapted from ref. 24. The positions of glycine and two of the three sodium ions are depicted by a yellow triangle and blue circles, respectively. (**c**) Alignment of the TM6–TM7 region of GlyT2 with other Na^+/Cl^--dependent neurotransmitter transporters shows that residue Trp482 is only found at the equivalent position in GlyT1 and GlyT2, whereas Tyr491 and Asn509 are highly conserved throughout this superfamily. Residue Ser510 is conserved in taurine, GABA and dopamine transporters.

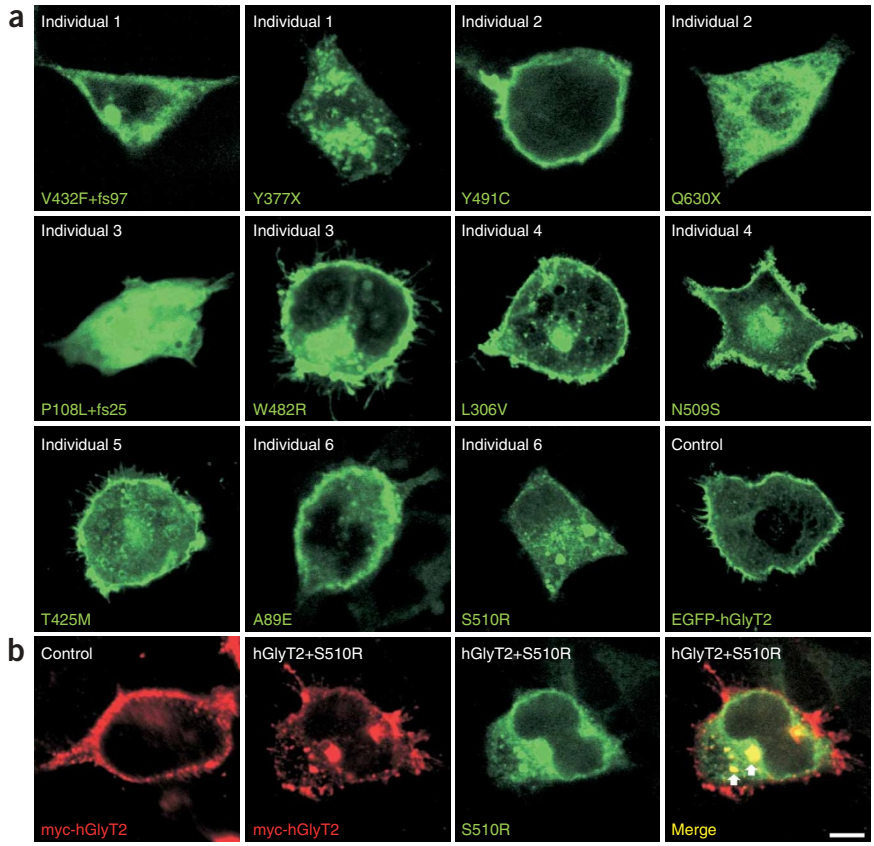

Figure 2 Subcellular localization of EGFP-hGlyT2 and hyperekplexia mutants. (**a**) Confocal microscopy of transfected HEK293 cells showing subcellular localization of EGFP-hGlyT2 and single hyperekplexia mutants and the A89E variant. Note that all mutants show distinct expression at the cell surface except P108L+fs25, Y377X, V432F+fs97, Q630X and S510R, which are cytoplasmic. (**b**) Coexpression experiments show that whereas myc-tagged hGlyT2 is expressed at the cell surface (left panel), mutant S510R traps myc-tagged hGlyT2 in intracellular aggregates (arrows in merged image). Scale bar, 10 μm.

disposition. However, the Y377X-causing paternal allele did not evoke a hyperekplectic phenotype. Compound heterozygosity in individual 2 consisted of nonsense and missense mutations resulting in the substitutions Q630X and Y491C, respectively. The origin of these alleles could not be determined in the unaffected parents because they had declined to participate in this study. However, long-distance PCR from exons 9 and 13 and subsequent cloning of PCR products showed that these alleles resided on different chromosomes. Individual 3 represents two sibling brothers with hyperekplexia; both inherited missense plus frameshift and missense mutations (resulting in the alterations P108L+fs25 and W482R, respectively) from their unaffected parents. Individual 4 inherited two missense mutations resulting in the substitutions L306V and N509S; individual 5 was homozygous for a single missense mutation (resulting in the substitution T425M) inherited from consanguineous parents. Finally, a maternal missense mutation (resulting in the substitution S510R) was identified in individual 6. Although a paternal sequence variation (A89E) was identified, we were able to exclude the possibility of compound heterozygosity because this variant was also detected in 4 of 203 control samples. All individuals with mutations in *SLC6A5* presented with classical symptoms of hyperekplexia (see **Supplementary Note** and **Supplementary Video 1** (for individual 6) online), including neonatal muscle hypertonia and an exaggerated startle response to tactile or acoustic stimuli with preservation of consciousness. However, in contrast to most individuals with mutations in *GLRA1*, individuals with *SLC6A5* mutations showed prolonged spasms with life-threatening neonatal apnea and breath-holding episodes. Notably, in some cases, symptoms resolved in the first year of life.

To confirm the pathogenicity of these alleles, we performed a series of functional tests using recombinant expression of human GlyT2 and mutants produced by site-directed mutagenesis. These experiments included assessment of cell-surface localization and capacity for [^{3}H]glycine uptake in HEK293 cells, together with electrophysiological measurements of glycine-evoked steady-state currents in *Xenopus laevis* oocytes. Non-mutated EGFP- or myc-tagged hGlyT2 as well as A89E, L306V, T425M, W482R, Y491C and N509S mutants were readily expressed at the cell surface (**Fig. 2a**). By contrast, frameshift (P108L+fs25 and V432F+fs97) and nonsense (Y377X and Q630X) mutant proteins were clearly cytoplasmic, suggesting that protein truncation resulted in a loss of cell surface GlyT2. The S510R mutant protein was also cytoplasmic, but it formed intracellular aggregates (**Fig. 2a**,**b**) that readily trapped cotransfected myc-tagged hGlyT2 (**Fig. 2b**), supporting a dominant-negative mode of action. Consistent with these findings, substitutions P108L+fs25, Y377X, V432F+fs97, Q630X and S510R abolished [^{3}H]glycine uptake (**Fig. 3a**). Despite reaching the cell surface, transporters with substitutions T425M, W482R, Y491C and N509S also showed no significant [^{3}H]glycine uptake, whereas those with A89E and L306V resembled EGFP-hGlyT2 (**Fig. 3a**). Taken together, these data provide strong evidence for a biallelic loss of GlyT2 function in individuals 1 (Y377X plus V432F+fs97), 2 (Q630X plus Y491C), 3 (P108L+fs25 plus W482R) and 5 (T425M, homozygous). However, the mechanisms underlying the clinical phenotype in individuals 4 (L306V plus N509S) and 6 (heterozygous for S510R) remained ambiguous. We therefore tested whether cotransfection of the two alleles would provide evidence for dominant or synergistic effects, as intracellular heteromeric GlyT2 assembly has been reported, although cell-surface GlyT2 is presumed to be monomeric[23]. Mixing N509S or L306V with EGFP-hGlyT2 did not substantially alter [^{3}H]glycine uptake, but mixing N509S with L306V completely abolished uptake (**Fig. 3b**). This indicates that *in vivo*, N509S and L306V mutant polypeptides may act synergistically to cause biallelic GlyT2 dysfunction, compatible with a recessive mode of inheritance. Consistent with cytoplasmic trapping of myc-tagged GlyT2 by EGFP-hGlyT2S510R (**Fig. 2b**), coexpression of S510R with hGlyT2 or A89E resulted in the loss of [^{3}H]glycine uptake (**Fig. 3b**), providing further evidence that the mutation producing the S510R substitution is dominant negative.

Insights into the precise molecular mechanisms underlying mutations in *SLC6A5* were provided by homology modeling of GlyT2 using the crystal structure of the bacterial leucine transporter (LeuT; ref. 24). Alignment of the *Aquifex aeolicus* LeuT with GlyT1 and GlyT2 allowed

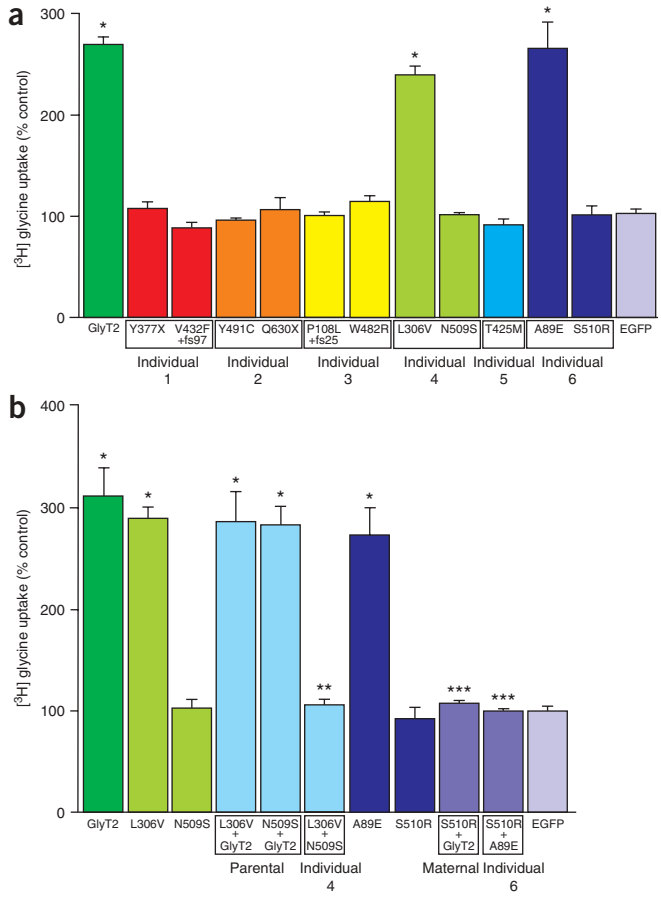

Figure 3 Transport activity of hGlyT2 and hyperekplexia mutants. (**a**) Glycine uptake in HEK293 cells transiently expressing EGFP-hGlyT2 or single hyperekplexia mutants after incubation with [^{3}H]glycine. (**b**) Selected pairwise mutant combinations and controls. Because low levels of endogenous glycine uptake are found in HEK293 cells[30], [^{3}H]glycine uptake was expressed as a percentage of that in control cells transfected with pEGFP-C1 (empty expression vector; EGFP). Data are given as means ± s.e.m. (n = 6–20). * significantly different from EGFP, ** significantly different from L306V, *** significantly different from GlyT2 or A89E; $P < 0.01$.

us to identify residues potentially involved in coordinating glycine and Na^+ binding. In particular, we predicted that alterations W482R (TM6) and N509S (TM7) could disrupt the binding to GlyT2 of glycine or Na^+, respectively (**Fig. 1a–c**).

Two-electrode voltage-clamp analysis in *Xenopus* oocytes demonstrated that the mutant W482R does not respond to glycine (up to 10 mM). However, the mutant W482R was clearly present at the cell surface, as demonstrated by Na^+-dependent transient currents[9,25] that were glycine insensitive but blocked by the drug ORG25543 (a specific GlyT2 inhibitor; **Fig. 4a–c**). By contrast, neither transient nor glycine-induced currents could be detected for mutants T425M, Y491C or S510R. This confirmed our prior [^{3}H]glycine uptake results (**Fig. 3a**) and indicated that although T425M and Y491C reach the cell surface (**Fig. 2a**), they may not be functional. Transient and steady-state currents, which are related to transporter expression[26,27], were observed for L306V and for N509S. However, disruption of the highly conserved residue N509 produced a marked and voltage-dependent decrease in glycine potency (**Fig. 4b–c**) from a half-maximal effector concentration (EC_{50}) of 26.9 ± 3.3 μM (hGlyT2) to 1,920 ± 230 μM (N509S) at –40 mV (**Fig. 4c**). Similar results were obtained for glycine-activated currents for hGlyT2 and N509S expressed in NG108 cells (**Supplementary Fig. 2** online; EC_{50} at –50 mV for hGlyT2, 27.4 ± 2.4 μM; for N509S, 2,650 ± 420 μM). These shifts in potency were sufficient to account for the apparent lack of glycine uptake for N509S in HEK293 cells (**Fig. 3a**; assayed using 200 μM glycine) and demonstrated that although N509S may impair Na^+-glycine coupling, alteration L306V alone did not substantially impair transporter function. Current-voltage relationships for N509S and L306V in oocytes were similar to that for hGlyT2, showing that these mutants conserved a high thermodynamic coupling between glycine-evoked current and glycine uptake (**Fig. 4d**). We assessed the charge movement (Q_v) across the oocyte membrane associated with the activation of GlyT2 by measuring the integrals of the transient currents at different voltage-clamp holding potentials (V_m). Fitting the resulting $Q_v - V_m$ relationships to the Boltzmann equation showed that all possessed similar equivalent charges (zδ) to hGlyT2, indicating no difference in the number of Na^+ ions that are bound to the transporter. However, the holding potential at which the charge transfer is half the maximum ($V_{0.5}$) for all three GlyT2 mutants was shifted to hyperpolarized potentials, in accord with a reduced apparent affinity for Na^+ (**Fig. 4e**).

In conclusion, it is apparent that hyperekplexia is principally caused by defects in glycinergic transmission that conspire to alter either postsynaptic receptor function or location or, alternatively, presynaptic vesicular replenishment. Although mouse knockouts for GlyT2 have been suggested[15] to show a behavioral phenotype similar to human hyperekplexia, there are several marked differences from individuals with mutations in *SLC6A5*. GlyT2 knockout mice gain weight slowly and die prematurely at the end of the second postnatal week, showing a complex neurological phenotype characterized by spasticity, a severely impaired righting reflex and, of particular note, rigid muscle tone and strong spontaneous tremor. By contrast, humans with mutations in *SLC6A5* show no spontaneous tremor or muscle stiffness, although these can be triggered by acoustic or tactile stimuli.

Our results demonstrate that *SLC6A5* is a major gene for hyperekplexia and define the first neurological disorder linked to alterations in a Na^+/Cl^--dependent transporter for a classical fast neurotransmitter. By analogy, we suggest that in other human disorders where defects in postsynaptic receptors have been identified, similar symptoms could result from defects in the cognate presynaptic neurotransmitter transporter. In the hierarchical genetic analysis of hyperekplexia, *SLC6A5* must now be regarded as an important candidate gene and have equal priority to *GLRA1* in screening. GlyT2 accessory proteins (such as the PDZ-domain-containing protein syntenin-1 and ULIP6) that are involved in the correct localization of GlyT2 at presynaptic terminals[28,29] must also be considered as candidates for the remaining individuals with hyperekplexia awaiting a definitive genetic diagnosis. Finally, although mutations in *SLC6A5* should be regarded as a risk factor for sudden infant death syndrome, owing to developmentally specific anoxic seizures and cyanotic syncope, symptoms often resolve during the transient developmental period from early postnatal months into infancy.

METHODS

Mutation screening of the human GlyT2 gene (*SLC6A5*). We screened 83 samples, all of which had proved gene-negative in screens[3–6] of *GLRA1*, *GLRB*, *GPHN* and *ARHGEF9*, for *SLC6A5* mutations. Four samples came from two sets of asymptomatic parents of affected children and three others came from members of a large family with one severely affected individual. The remaining

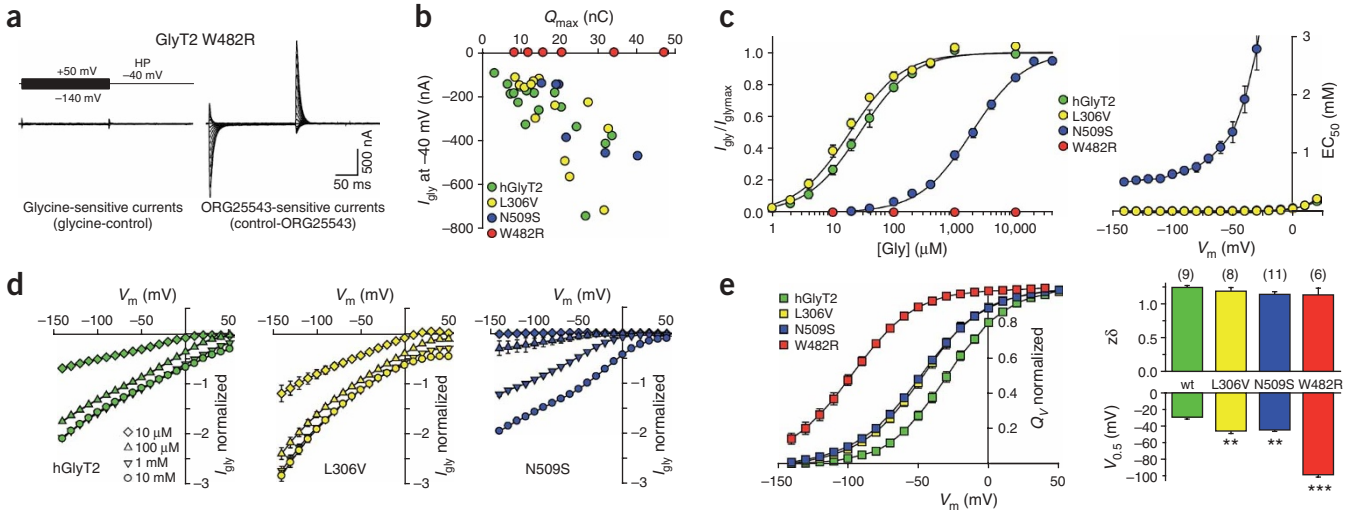

Figure 4 Electrophysiological characterization of hGlyT2 mutants. (**a**) Steady-state (I_{gly}) and transient currents of W482R are insensitive to glycine (10 mM, left) whereas ORG25543 (5 μM) blocked Na^+-dependent transient currents (right). HP, holding potential. (**b**) Plot of I_{gly} (–40 mV) and ORG25543-sensitive charge movement relationship for hGlyT2 and mutants. We evoked I_{gly} with applications of 1 mM (hGlyT2, L306V) or 10 mM (N509S, W482R) glycine. We obtained Q_{max} values as described below. (**c**) Left, glycine dose-response curves of I_{gly} for hGlyT2 and mutants. EC_{50} values were 26.9 ± 3.3 μM (hGlyT2), 18.8 ± 1.5 μM (L306V) and 1,920 ± 230 μM (N509S) at –40 mV and 22.5 ± 3.15 μM (hGlyT2), 15.9 ± 1.2 μM (L306V) and 913 ± 72.2 μM (N509S) at –70 mV. We fitted curves with the equation $I_{gly} = I_{glymax}/(1 + EC_{50}/[gly])$ and normalized them to I_{glymax} ($n = 3$–5). Right, plot of glycine EC_{50}-V_m relationship for hGlyT2 and mutants. (**d**) Normalized I_{gly} – V_m curves for hGlyT2 and mutants. I_{gly} were normalized to the 10-mM-glycine–evoked currents recorded at –40 mV ($n = 3$–7). (**e**) Left, normalized Q_{Vm} – V_m relationships for hGlyT2 and mutants. Q_{Vm} are the time integrals of ORG25543-sensitive transient currents. We fitted Q_{Vm} – V_m curves to the Boltzmann equation $Q_{Vm} = Q_{min} + Q_{max}/[1 + \exp(0.03\ z\delta\ (V_{0.5} - V_m))]$ and normalized them to Q_{max}. Right, histograms of the mean zδ (top) and $V_{0.5}$ (bottom) for hGlyT2 and mutants. zδ values were 1.25 ± 0.02 (hGlyT2), 1.20 ± 0.05 (L306V), 1.15 ± 0.04 (N509S) and 1.14 ± 0.1 (W482R); $V_{0.5}$ values were –29.3 ± 2.44 (hGlyT2), –46.4 ± 2.7 (L306V), –44.8 ± 1.25 (N509S) and –98.6 ± 2.75 (W482R). Statistical comparisons were made using a paired *F*-test. $^{**}P < 0.01$; $^{***}P < 0.001$; means ± s.e.m. are shown; number of oocytes is in parentheses).

76 samples all came from unrelated individuals with sporadic cases from neurological or genetics clinic referrals. Ethical approval for the genetic testing of individuals with epilepsy and paroxysmal disorders is held with the Auckland Regional Ethical Committee in New Zealand (M.I.R.). The referring clinicians hold written consent from participants or parents for blood sample collection and genetic screening in accordance with individual national ethical requirements. Separate parental consent was obtained to publish **Supplementary Video 1**. Participant and physician written consent was a study prerequisite, but because of the multinational origin of DNA samples, the consent format was not standardized. We derived *SLC6A5* exons, flanking intronic sequences and 5′ and 3′ untranslated regions *in silico*, using the Human Genome Browser at UCSC. We amplified participant genomic DNA using PCR primers described in **Supplementary Table 1**. Each 25 μl reaction contained 60 ng of genomic DNA, 10 pmol of each primer, 1.5 mM $MgCl_2$, 50 mM KCl, 10 mM Tris-HCl buffer, pH 8.3, 200 μM dNTPs and 1 U *Taq* polymerase (Qiagen). PCR conditions were 94 °C for 5 min followed by 35 cycles of 30 s at 94 °C, 30 s at 60 °C and 30 s at 72 °C. We screened PCR products for SNPs and other mutations using a dHPLC HT-WAVE DNA Fragment Analysis System with DNASep columns (Transgenomic) under partially denaturing conditions. For samples showing aberrant dHPLC profiles, we isolated the DNA from gels (QIAGEN) and sequenced it using ABI3100 and BigDye ready reaction technology (Applied Biosystems). We screened population samples using RFLPs or, in the absence of a restriction site assay, analyzed dHPLC profiles of controls with a mutation-positive sample.

Amplification, cloning and mutagenesis of human GlyT2 cDNAs. We amplified human GlyT2 cDNAs from human hippocampal cDNA (Clontech) using the primers hGlyT2A-1 and hGlyT2A-2 (**Supplementary Table 1** online) and 30 cycles of 94 °C for 1 min, 60 °C for 1 min and 68 °C for 6 min. We cloned PCR products into the *Eco*RI and *Xho*I sites of the vector pcDNA3 (Invitrogen) and sequenced 12 full-length cDNAs. hGlyT2-1 encodes Gly102, Ser124, Lys457 and Asp463 (**Supplementary Table 3** online). We subcloned the insert from one of these clones, pcDNA3-hGlyT2-1, into three more vectors: pEGFP-C1 (Clontech; resulting in construct pEGFP-hGlyT2, N-terminal EGFP tag), pRK5myc (resulting in construct pRK5myc-GlyT2, N-terminal myc tag) and pRC/CMV (Invitrogen; resulting in plasmid pRC/CMV-hGlyT2). Then we introduced *SLC6A5* mutations into these plasmids using the QuikChange site-directed mutagenesis kit (Stratagene). We sequenced the full coding region of each construct as above to verify that only the desired mutation had been introduced.

Glycine uptake assays. We plated HEK293 cells (ATCC CRL1573) onto poly-D-lysine-coated 24-well plates (Nunc) and grew them to 50% confluence in MEM (Earles salts) supplemented with 10% (vol/vol) FCS, 2 mM L-glutamine and 20 U/ml penicillin-streptomycin in 5% CO_2–95% air. We transfected them with 0.25 μg total pEGFP-C1 (control), pEGFP-hGlyT2 or mutant DNAs per well using Effectene (Qiagen). After 24 h, we washed the cells with a buffer containing 116 mM NaCl, 1 mM NaH_2PO_4, 26 mM $NaHCO_3$, 1.5 mM $MgSO_4$, 5 mM KCl, 1.3 mM $CaCl_2$ and 5 mM glucose pre-equilibrated with 5% CO_2–95% air, then incubated them for 5 min in 1 μCi/ml [^{3}H]glycine (60 Ci/mmol, NEN) at a final concentration of 200 μM. Two additions of ice-cold buffer followed by aspiration terminated the uptake. We then digested cells in 0.1 M NaOH and used these samples for scintillation counting and for determination of protein concentration using Bradford reagent (Bio-Rad). [^{3}H]glycine uptake was calculated as nanomoles per minute per milligram of protein (nmol/min/mg protein) and expressed as a percentage of that in control cells transfected with pEGFP-C1 (which was 0.46 nmol/min/mg protein; $n = 20$). To determine the kinetics of [^{3}H]glycine uptake, we used cells expressing pEGFP-hGlyT2 in the presence of 1–1,000 μM unlabeled glycine. This showed a K_m of 66 μM and V_{max} of 1.64 nmol/min/mg protein. All statistical comparisons used an unpaired Student's *t*-test.

GlyT2 subcellular localization. We electroporated HEK293 cells (400 V, infinite resistance, 125 μF; BioRad Gene Electropulser II) with pEGFP-hGlyT2 (wild-type) or mutant plasmids. After 24 h, we washed the cells twice in PBS, fixed for 5 min in 4% (wt/vol) PFA in PBS and quenched in 50 mM NH_4Cl for

10 min before further washing in PBS. For confocal microscopy we used a Zeiss Axioscop LSM 510 Meta confocal microscope with 40× objective (NA 1.3) and 3× digital zoom. We acquired images (1,024×1,024 pixel resolution) after laser excitation (488 nm) of a 0.9-μm optical section and stored them for further analysis. We transfected each mutant at least four times and obtained images from at least four cells per mutant. Phenotypes shown were present in >85% of transfected cells. Cells showing extreme levels of exogenous protein expression, obvious cell volume loss or other signs of cell death were discounted from image analysis.

Electrophysiological analysis of GlyT2 mutants. We prepared *Xenopus* oocytes as previously described[9]. We synthesized mRNAs coding for wild-type GlyT2 and each mutant *in vitro* from pRC/CMV-hGlyT2 constructs (mMessage-mMachine, AMBION) and injected ~50 ng of mRNA into each *Xenopus* oocyte. Three to seven days after mRNA injection, we held the oocyte at –40 mV with a two-microelectrode voltage-clamp amplifier (WARNER OC725C) while continuously perfusing with Ringer's solution (100 mM NaCl, 1.8 mM $CaCl_2$, 1 mM $MgCl_2$, 5 mM HEPES buffer, adjusted to pH 7.4 with KOH). We filtered the currents at 1 kHz before digitizing them at 5 kHz (Digidata 1200 or 1320A, Axon Instruments, PClamp 8).

We grew NG108-15 cells under nondifferentiating conditions in MEM (Earles salts) with 10% (vol/vol) FCS, 4 mM L-glutamine, 1.13% (wt/vol) glucose, 20 U/ml penicillin-streptomycin and 2% HAT media supplement (50×) in 5% CO_2–95% air. We plated cells onto polyornithine-coated coverslips and transfected them with cDNAs for GlyT2 and EGFP using calcium phosphate. Up to 16 h later (at 20–22 °C), we recorded whole-cell glycine-evoked currents, normalized to cell capacitance, from single NG108 cells voltage clamped at –50 mV using an Axopatch 200B (Axon Instruments) and filtered the currents (8-pole Bessel) at 2 kHz before digitizing them (Digidata 1320A). Patch electrodes (3–5 MΩ) contained 140 mM potassium gluconate, 1 mM $MgCl_2$, 1 mM $CaCl_2$, 11 mM EGTA, 5 mM ATP and 10 mM HEPES, pH 7.2. Krebs solution for continuous superfusion contained 140 mM NaCl, 4.7 mM KCl, 1.2 mM $MgCl_2$, 2.5 mM $CaCl_2$, 11 mM glucose and 10 mM HEPES, pH 7.4. We applied all solutions using a modified U-tube. We analyzed the data using Clampfit 8.2 (Axon) and Origin 6 (Microcal). Dose-response relationships we fitted with the Hill equation. All data points represent the mean ± s.e.m.

Requests for materials. Requests for materials are subject to a Material Transfer Agreement.

URLs. UCSC Genome Browser: http://genome.ucsc.edu/.

Note: Supplementary information is available on the Nature Genetics website.

ACKNOWLEDGMENTS

We thank E.A. Peeters and K. Braun for referrals of research participants. This work was supported by grants from the Medical Research Council (UK) to R.J.H. and T.G.S., from the Neurological Foundation for New Zealand and Auckland Medical Research Foundation to M.I.R. and from the Fédération pour la Recherche sur le Cerveau and the Association Française contre les Myopathies to S.S.

COMPETING INTERESTS STATEMENT

The authors declare that they have no competing financial interests.

Published online at http://www.nature.com/naturegenetics
Reprints and permissions information is available online at http://npg.nature.com/reprintsandpermissions/

1. Shiang, R. *et al.* Mutations in the α1 subunit of the inhibitory glycine receptor cause the dominant neurologic disorder, hyperekplexia. *Nat. Genet.* **5**, 351–358 (1993).
2. Shiang, R. *et al.* Mutational analysis of familial and sporadic hyperekplexia. *Ann. Neurol.* **38**, 85–91 (1995).
3. Rees, M.I. *et al.* Compound heterozygosity and nonsense mutations in the α1-subunit of the inhibitory glycine receptor in hyperekplexia. *Hum. Genet.* **109**, 267–270 (2001).
4. Rees, M.I. *et al.* Hyperekplexia associated with compound heterozygote mutations in the β-subunit of the human inhibitory glycine receptor (*GLRB*). *Hum. Mol. Genet.* **11**, 853–860 (2002).
5. Rees, M.I. *et al.* Isoform heterogeneity of the human gephyrin gene (*GPHN*), binding domains to the glycine receptor, and mutation analysis in hyperekplexia. *J. Biol. Chem.* **278**, 24688–24696 (2003).
6. Harvey, K. *et al.* The GDP-GTP exchange factor collybistin: an essential determinant of neuronal gephyrin clustering. *J. Neurosci.* **24**, 5816–5826 (2004).
7. Vergouwe, M.N. *et al.* Hyperekplexia-like syndromes without mutations in the *GLRA1* gene. *Clin. Neurol. Neurosurg.* **99**, 172–178 (1997).
8. Morrow, J.A. *et al.* Molecular cloning and functional expression of the human glycine transporter GlyT2 and chromosomal localisation of the gene in the human genome. *FEBS Lett.* **439**, 334–340 (1998).
9. Roux, M.J. & Supplisson, S. Neuronal and glial glycine transporters have different stoichiometries. *Neuron* **25**, 373–383 (2000).
10. Eulenburg, V., Armsen, W., Betz, H. & Gomeza, J. Glycine transporters: essential regulators of neurotransmission. *Trends Biochem. Sci.* **30**, 325–333 (2005).
11. Supplisson, S. & Roux, M.J. Why glycine transporters have different stoichiometries. *FEBS Lett.* **529**, 93–101 (2002).
12. Gabernet, L. *et al.* Enhancement of the NMDA receptor function by reduction of glycine transporter 1 expression. *Neurosci. Lett.* **373**, 79–84 (2005).
13. Gomeza, J. *et al.* Inactivation of the glycine transporter 1 gene discloses vital role of glial glycine uptake in glycinergic inhibition. *Neuron* **40**, 785–796 (2003).
14. Tsai, G. *et al.* Gene knockout of glycine transporter 1: characterization of the behavioral phenotype. *Proc. Natl. Acad. Sci. USA* **101**, 8485–8490 (2004).
15. Gomeza, J. *et al.* Deletion of the mouse glycine transporter 2 results in a hyperekplexia phenotype and postnatal lethality. *Neuron* **40**, 797–806 (2003).
16. Krogsgaard-Larsen, P., Frolund, B. & Frydenvang, K. GABA uptake inhibitors. Design, molecular pharmacology and therapeutic aspects. *Curr. Pharm. Des.* **6**, 1193–1209 (2000).
17. Barker, E.L. & Blakely, R.D. Norepinephrine and serotonin transporters: molecular targets of antidepressant drugs. In *Psychopharmacology—the Fourth Generation of Progress* (eds. Bloom, F.E. & Kupfer, D.J.) 321–333 (Raven, New York, 1995).
18. Hahn, M.K. & Blakely, R.D. Monoamine transporter gene structure an polymorphisms in relation to psychiatric and other complex disorders. *Pharmacogenomics J.* **2**, 217–235 (2002).
19. Hahn, M.K., Mazei-Robison, M.S. & Blakely, R.D. Single nucleotide polymorphisms in the human norepinephrine transporter gene affect expression, trafficking, antidepressant interaction, and protein kinase C regulation. *Mol. Pharmacol.* **68**, 457–466 (2005).
20. Richerson, G.B. & Wu, Y. Role of the GABA transporter in epilepsy. *Adv. Exp. Med. Biol.* **548**, 76–91 (2004).
21. Hahn, K.A. *et al.* X-linked mental retardation with seizures and carrier manifestations is caused my mutation in the creatine-transporter gene (*SLC6A8*) located in Xq28. *Am. J. Hum. Genet.* **70**, 1349–1356 (2002).
22. Rosenberg, E.H. *et al.* High prevalence of *SLC6A8* deficiency in X-linked mental retardation. *Am. J. Hum. Genet.* **75**, 97–105 (2004).
23. Horiuchi, M. *et al.* Surface-localized glycine transporters 1 and 2 function as monomeric proteins in *Xenopus* oocytes. *Proc. Natl. Acad. Sci. USA* **98**, 1448–1453 (2001).
24. Yamashita, A., Singh, S.K., Kawate, T., Jin, Y. & Gouaux, E. Crystal structure of a bacterial homologue of Na^+/Cl^--dependent neurotransmitter transporters. *Nature* **437**, 215–223 (2005).
25. Roux, M.J. *et al.* The glial and the neuronal glycine transporters differ in their reactivity to sulfhydryl reagents. *J. Biol. Chem.* **276**, 17699–17705 (2001).
26. Mager, S. *et al.* Steady states, charge movements, and rates for a cloned GABA transporter expressed in *Xenopus* oocytes. *Neuron* **10**, 177–188 (1993).
27. Mager, S. *et al.* Ion binding and permeation at the GABA transporter GAT1. *J. Neurosci.* **16**, 5405–5414 (1996).
28. Ohno, K. *et al.* The neuronal glycine transporter 2 interacts with the PDZ domain protein syntenin-1. *Mol. Cell. Neurosci.* **26**, 518–529 (2004).
29. Horiuchi, M., Loebrich, S., Brandstaetter, J.H., Kneussel, M. & Betz, H. Cellular localization and subcellular distribution of Unc-33-like protein 6, a brain-specific protein of the collapsing response mediator protein family that interacts with the neuronal glycine transporter 2. *J. Neurochem.* **94**, 307–315 (2005).
30. Tunnicliff, G. Membrane glycine transport proteins. *J. Biomed. Sci.* **10**, 30–36 (2003).